Stable motion Path of airborne charged Particles by large Charges on the Earth's surface （ Formation of two type Seismic Clouds ）

Fumitaka Inuyama, Senior Power Engineer (e-mail: inusanin@yahoo.co.jp)
Permanent address: 5-17-33 Torikai Jonan, Fukuoka City, 814-0103, Japan
Thermal Power Dept., Kyushu Electric Power Co., Inc.(www.kyuden.co.jp) (Retired)

Introduction

As phenomena that occur before an earthquake : 1) Ground elevation, horizontal distortion, and inclination, 2) Abnormalities in seismic activity (foreshocks, blank areas, etc.) and changes in seismic activity areas, 3) Changes in geomagnetism, ground current, electric field, and electrical resistance, 4) Changes in well water (spring water volume, pollution, fine sand contamination, radon concentration and chlorine content etc.), 5) Abnormalities and luminescence phenomena of electromagnetic radiation, 6) Abnormal behavior of animals, birds and beasts, and insects. It seems that events such as are occurring.[1] [2]

As a factor in luminescence phenomena and changes in geomagnetism, ground current, and electric fields, which are precursors to large-scale earthquakes, a mechanism has been proposed in which a free charge is generated in the crust when pressure is applied to the bedrock of the earth's crust, which appears on the ground surface and generates a ground surface charge, which also has an electrical impact on the sky. [3] [4] [5]. The presence of a large number of electrically charged aerosols and liquid microscopic water droplets floating in the air can also be seen by the rainbow in the desert. Thus, it is clear that a large charge on the earth's surface exerts a Coulomb force on charged particles suspended in the air and the stable motion path of airborne charged particles (i.e. microscopic water droplets coexisting with water vapor) is elucidated based on the principle of minimum mechanical energy, and the formation of seismic clouds is studied.

1. Coulomb force of point charge

1-1. Equations of motion of charged particles

The earth's surface is defined as the x-y plane, the downwind direction of the horizontal wind is the x axis, the vertical direction is the z axis, the coordinates of the particles is (x, y, z), the wind speed is $(V_x,\ 0, V_z)$, there is a large charge Q'at coordinate origin, and the charge of the airborne charged particles is defined q . The equations of motion in the x,y,z directions of a charged particle taking into account the inertial force, viscous drag, Coulomb force, gravity and buoyancy acting on relative motion particles in the air flow are as follows.

However, the viscous drag D of air is expressed as proportional to $\mathbf{v}^{\mathbf{n}}$ or $f(\mathbf{v})$ here, because there are Stokes' law D= 3 $\pi\mu$ **v** d , which holds for the small Reynolds number （Re= v d/ν） of the particle and the fluid drag D=C_D ・ 1/2ρ **v** ²A. (The drag coefficient C_D depends on Re. Fig. 1). Note that the induced mass of an object moving at an accelerated motion in a fluid is ignored.

$$m\frac{d}{dt}\left(\frac{dx}{dt}-V_x(z)\right)+\ C(z)\left(\frac{dx}{dt}-V_x(z)\right)^n+\frac{Q'q}{4\pi\varepsilon_o\varepsilon_r}\cdot\frac{\partial}{\partial x}\left[\frac{1}{\sqrt{x^2+y^2+z^2}}\right]=0$$

$$m\frac{d^2y}{dt^2}+C(z)\left(\frac{dy}{dt}\right)^n+\frac{Q'q}{4\pi\varepsilon_o\varepsilon_r}\cdot\frac{\partial}{\partial y}\left[\frac{1}{\sqrt{x^2+y^2+z^2}}\right]=0$$

$$m\frac{d}{dt}\left(\frac{dz}{dt}-V_z(z)\right)+\ C(z)\left(\frac{dz}{dt}-V_z(z)\right)^n+\left(m-\frac{4\pi r^3\rho(z)}{3}\right)g+\frac{Q'q}{4\pi\varepsilon_o\varepsilon_r}\cdot\frac{\partial}{\partial z}\left[\frac{1}{\sqrt{x^2+y^2+z^2}}\right]=0$$

If the symbol is simplified as follows, the equations of motion in the direction x, y, z are (Eq. 1) ~ (Eq. 3).

$$Q = \frac{Q'q}{4\pi\varepsilon_o\varepsilon_r}, \quad G(z) = \left(m - \frac{4\pi r^3\rho(z)}{3}\right)g \ , \quad R = \sqrt{x^2+y^2+z^2}$$

(1) $$m\frac{d}{dt}\left(\frac{dx}{dt} - V_x(z)\right) + C(z)\left(\frac{dx}{dt} - V_x(z)\right)^n - Q\cdot\frac{x}{R^3} = 0$$

(2) $$m\frac{d^2y}{dt^2} + C(z)\left(\frac{dy}{dt}\right)^n - Q\cdot\frac{y}{R^3} = 0$$

(3) $$m\frac{d}{dt}\left(\frac{dz}{dt} - V_z(z)\right) + C(z)\left(\frac{dz}{dt} - V_z(z)\right)^n + G(z) - Q\cdot\frac{z}{R^3} = 0$$

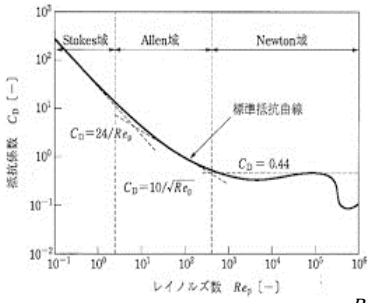

Fig. 1 Drag coefficient of sphere Re

The above equations are two-order ordinary differential equations of a three-way coalition, and it is considered realistically difficult to solve analytically using algebra.

Measurement examples of altitude changes in viscosity μ, density ρ, and wind speed V_x are shown in (Fig. 2) ~ (Fig. 4).

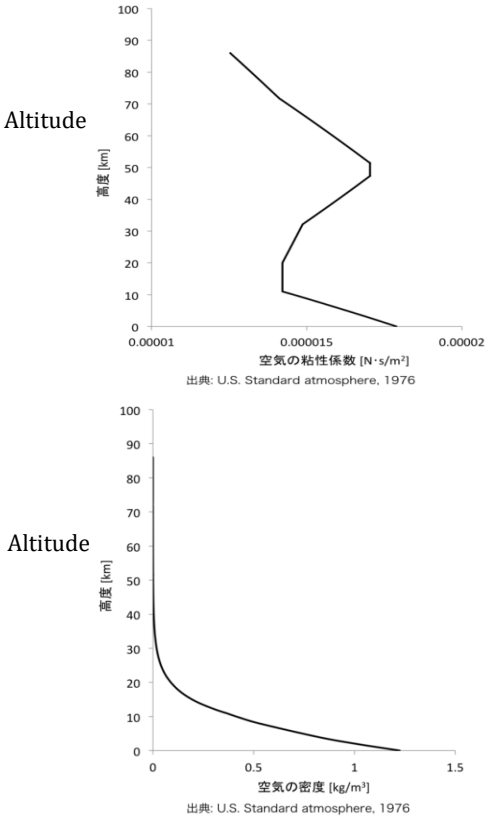

Fig. 2, 3 Viscosity μ and density ρ of air vs altitude［6］

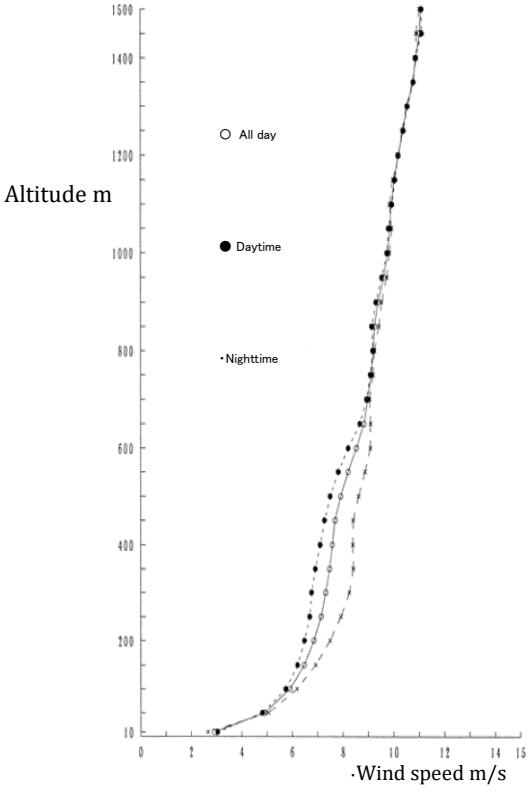

Fig. 4 Wind speed distribution by altitude［7］

Since the air density ρ is a function of the altitude z, the viscosity term $C(z)$ and the gravity term $G(z)$ are first approximated. The same applies to wind speed and adopt the coefficients according to altitude.

$C(z) = -az + b$, $G(z) = \alpha z + \beta$ ($a, b, \alpha, \beta > 0$ 、z < 10,000m)

$V_x(z) = \varepsilon z + V_{x0}$, $V_z(z) = -\eta z + V_{z0}$ ($\varepsilon, \eta > 0$)

If it examines the equation of motion of (Eq. 1) ~ (Eq. 3)

① From (Eq. 2) it is an even function of y in case of n=1,3,5 . （y=−Y is the same function as (Eq. 2)）
From (Eq. 2) **y=0 is a singular solution.（y=0 holds for all domains of t ）**

② From (Eq. 1) in case of t=∞, it becomes $x = V_x\, t$

From (Eq. 2) in case of t=∞, it becomes $y = k_y$

From (Eq. 3) in case of t=∞, since z is in equilibrium $dz/dt = 0$, it becomes $\boldsymbol{C(z_e)V_z(z_e) = G(z_e)}$.

The equilibrium height z_e is the solutin of $a\eta\, {z_e}^2 - (aV_{z0} + b\eta + \alpha)\, z_e + (bV_{z0} - \beta) = 0$

If the solution of simultaneous differential equations are $x = x(t, k_1, \dots, k_6)$, $y = y(t, k_1, \dots, k_6)$ and $z = z(t, k_1, \dots, k_6)$, any integral constant k_i are determined by the initial positions and initial velocities etc. of the particle. Among the countless paths, ① and ② alone do not determine a specific energy stable path. Singular solutions of differential equations are also one of the countless paths.

1-2. Mechanical energy and dissipation energy

The dissipation energy E_D by air viscosity consumed from time to moment is expressed as follows.

$$E_D = \int C(z)\left(\frac{dx}{dt} - V_x(z)\right)^n \left(\frac{dx}{dt} - V_x(z)\right)dt + \int C(z)\left(\frac{dy}{dt}\right)^n \frac{dy}{dt}dt + \int C(z)\left(\frac{dz}{dt} - V_z(z)\right)^n \left(\frac{dz}{dt} - V_z(z)\right)dt$$

Mechanical energy E_M is expressed as (Eq. 4).

$$(4) \qquad E_M = \frac{m}{2}\left[\left(\frac{dx}{dt} - V_x(z)\right)^2 + \left(\frac{dy}{dt}\right)^2 + \left(\frac{dz}{dt} - V_z(z)\right)^2\right] + \int G(z)dz + Q/\sqrt{x^2 + y^2 + z^2}$$

Since the motion of an object is based on the principle of mechanical energy minimum (in other words, maximum dissipation energy and increase in thermodynamic entropy), objects with unstable energies deviate from their paths due to slight disturbances and gradually become close to paths with low energy.

From the mechanical energy equation, it can say the following.

③ From (Eq. 4) it is an even function of y. (y=−Y is the same function as (Eq. 4))

④ To minimize E_M, always x=constant, y=constant and R=small/large (Q=—/+) are advantageous.

As a result of ①～④, **the mechanical energy stable path is singular $\boldsymbol{y=0}$**. Also $\boldsymbol{x=V_x\, t}$, $\boldsymbol{z=z_e}$ **at** $\boldsymbol{t=\infty}$.

Since y=0, if the solution of the differential equation (Eq. 1) and (Eq. 3) are $x = x(t, k_1, k_2, k_5, k_6)$, $y = 0$, $z = z(t, k_1, k_2, k_5, k_6)$ then, any integral constant k_i is determined by the initial positions and initial velocities etc. of the particle, and there are an infinite number of paths. On the other hand, if the initial conditions in the mechanical energy stable path are $x = x_0$, $dx/dt = v_{x0}$, $z = z_0$, $dz/dt = v_{z0}$ at $t = t_0$, then, it is expressed that the solutions of (Eq. 1) and (Eq. 3) are $x = x(t, x_0, v_{x0}, z_0, v_{z0})$, $y = 0$, $z = z(t, x_0, v_{x0}, z_0, v_{z0})$. The minimum mechanical energy conditions are as follows.

$$\frac{\partial E_M(t_0)}{\partial v_{x0}} = 0\ ;\ 2m(v_{x0} - V_x(z_0))\frac{\partial(v_{x0} - V_x(z_0))}{\partial v_{x0}} + 2m(v_{z0} - V_z(z_0))\frac{\partial(v_{z0} - V_z(z_0))}{\partial v_{x0}} + \frac{\partial}{\partial v_{x0}}\int G(z_0)dz_0 + \frac{\partial}{\partial v_{x0}}Q/\sqrt{{x_0}^2 + {z_0}^2} = 0$$

$$\frac{\partial E_M(t_0)}{\partial v_{z0}} = 0\ ;\ 2m(0 + v_{z0} - V_z(z_0)) + 0 + Q \cdot 0 = 0$$

$$\frac{\partial E_M(t_0)}{\partial x_0} = 0\ ;\ 2m(v_{x0} - V_x(z_0))\frac{\partial(v_{x0} - V_x(z_0))}{\partial x_0} + 2m(v_{z0} - V_z(z_0))\frac{\partial(v_{z0} - V_z(z_0))}{\partial x_0} + \frac{\partial}{\partial x_0}\int G(z_0)dz_0 + \frac{\partial}{\partial x_0}Q/\sqrt{{x_0}^2 + {z_0}^2} = 0$$

$$\frac{\partial E_M(t_0)}{\partial z_0} = 0\ ;\ 2m(0 + 0) + G(z_0) - Qz_0/({x_0}^2 + {z_0}^2)^{3/2} = 0$$

Consequently

$$v_{x0} = V_x(z_0)\ ,\quad v_{z0} = V_z(z_0)$$

$$x_0 = 0\ ,\qquad G(z_0)\,{z_0}^2 - Q = 0\quad (\alpha\,{z_0}^3 + \beta\,{z_0}^2 - Q = 0.\ \text{here, approximate to}\ G(z) = \alpha z + \beta\ )$$

From the above, **the stable path of the seismic cloud** which has the least mechanical energy, **is passing through $\boldsymbol{x_0 = 0}$, $\boldsymbol{y_0 = 0}$, $\boldsymbol{z_0}$** (z_0; solution of $2\alpha\,{z_0}^3 + \beta\,{z_0}^2 - Q = 0$) and **at $\boldsymbol{t \to \pm\infty}$ $\boldsymbol{x \to V_x(z_e)t \to \pm\infty}$, y=0, $\boldsymbol{z \to z_e}$** (z_e; equilibrium height solution of $C(z_e)\left(-V_z(z_e)\right)^n + G(z_e) = 0$)

1-3. Equations of motion at the time of calm

In the morning and evening when the weather is nice, the sea breeze and mountain breeze subside, so temporarily, it is $V_x = V_y = 0$. The equation of motion at the time of calm is as follows in polar coordinates, but it is difficult to solve rigorously.

$$radius\ \rho\ direction \quad m\frac{d^2\rho}{dt^2} + C(z)\left(\frac{d\rho}{dt}\right)^n - Q\cdot\frac{\rho}{R^3} = 0 \qquad \rho = \sqrt{x^2+y^2}\,, \quad R = \sqrt{x^2+y^2+z^2}$$

$$z\ direction \qquad m\frac{d}{dt}\left(\frac{dz}{dt} - V_z(z)\right) + C(z)\left(\frac{dz}{dt} - V_z(z)\right)^n + G(z) - Q\cdot\frac{z}{R^3} = 0$$

However, according to mathematical singular consideration, if there is no wind in the horizontal direction, the energy stable path is $x = y = 0$ ($\rho = 0$) and becomes a straight line rising vertically from the origin.

By balancing static forces in the z-axis direction, the equilibrium height z_e of the path is the solution of the following equation. If each coefficient is a first-order approximation and n = 1, it becomes a fourth-order equation of z_e. $\quad C(z_e)\left(-V_z(z_e)\right)^n + G(z_e) - Q/{z_e}^2 = 0$

1-4. Equations of motion at a distance

The approximate equation of motion at coordinates far from the origin ($|x| \gg z\ , y = 0$) is as follow. However, assuming that the change range z is small, $n = 1$, $C(z)$, $V_x(z)$, $V_z(z)$, $G(z)$ let to be constant.

$$m\frac{d^2x}{dt^2} + C\left(\frac{dx}{dt} - V_x\right) - Q\cdot\frac{1}{x^2} = 0 \qquad m\frac{d^2z}{dt^2} + C\left(\frac{dz}{dt} - V_z\right) + G - Q\cdot\frac{z}{x^3} = 0$$

Even in the above equation, since solving algebraically is a great amount of work [8], it can be solved by further omitting the Q term by micro-omission.

$$m\frac{d^2x}{dt^2} + C\left(\frac{dx}{dt} - V_x\right) = 0\ , \qquad m\frac{d^2z}{dt^2} + C\left(\frac{dz}{dt} - V_z\right) + G = 0$$

$$x = k_1\exp\left(-\frac{Ct}{m}\right) + V_x t + k_2\ , \qquad z = k_5\exp\left(-\frac{Ct}{m}\right) + \left(V_z - \frac{G}{C}\right)t + k_6$$

Thus, when t is larger, it is a horizontal strip of $x = V_x t + k_2$, $z = k_6$ and conforms to the result of §1-2.

2. Coulomb force of axisymmetric charge distribution

2-1. Equations of motion and mechanical energy of charged particles

Since the ground surface charge spreads with charge distribution on the ground surface rather than point charge Q', consider an axisymmetric charge distribution $\sigma'(r)$ like a normal distribution curve or a water surface pattern falling water droplet. In this case, the equations of motion of the charged particle are (eq. 1') ~ (eq. 3'), and the mechanical energy is (eq. 4').

(1′) $$m\frac{d}{dt}\left(\frac{dx}{dt} - V_x(z)\right) + C(z)\left(\frac{dx}{dt} - V_x(z)\right)^n - \int_0^\infty dr\int_0^{2\pi}\frac{x\,\sigma(r)\,r\ d\theta}{[(x-rcos\theta)^2 + (y-rsin\theta)^2 + z^2\,]^{3/2}} = 0$$

(2′) $$m\frac{d^2y}{dt^2} + C(z)\left(\frac{dy}{dt}\right)^n - \int_0^\infty dr\int_0^{2\pi}\frac{y\,\sigma(r)\,r\ d\theta}{[(x-rcos\theta)^2 + (y-rsin\theta)^2 + z^2\,]^{3/2}} = 0$$

(3′) $$m\frac{d}{dt}\left(\frac{dz}{dt} - V_z(z)\right) + C(z)\left(\frac{dz}{dt} - V_z(z)\right)^n + G(z) - \int_0^\infty dr\int_0^{2\pi}\frac{z\,\sigma(r)\,r\ d\theta}{[(x-rcos\theta)^2 + (y-rsin\theta)^2 + z^2\,]^{3/2}} = 0$$

(4′) $$E_M = \frac{m}{2}\left[\left(\frac{dx}{dt} - V_x(z)\right)^2 + \left(\frac{dy}{dt}\right)^2 + \left(\frac{dz}{dt} - V_z(z)\right)^2\right] + \int G(z)dz + \int_0^\infty dr\int_0^{2\pi}\frac{\sigma(r)\,r\ d\theta}{\sqrt{(x-rcos\theta)^2 + (y-rsin\theta)^2 + z^2}}$$

It transforms (Eq. 1') and (Eq. 2') to (Eq. 1'') and (Eq. 2''), here $sin\Phi = y/\sqrt{x^2+y^2}$

$$(1'') \quad m\frac{d}{dt}\left(\frac{dx}{dt} - V_x(z)\right) + C(z)\left(\frac{dx}{dt} - V_x(z)\right)^n - \int_0^{\infty} dr \int_0^{2\pi} \frac{[\, x - r\, cos\Phi\, cos(\theta - \Phi)\,]\, \sigma(r)\, r\ d\theta}{[x^2 + y^2 + z^2 + r^2 - 2r(x^2+y^2)^{1/2} cos(\theta - \Phi)]^{3/2}} = 0$$

$$(2'') \quad m\frac{d^2y}{dt^2} + C(z)\left(\frac{dy}{dt}\right)^n - \int_0^{\infty} dr \int_0^{2\pi} \frac{[\, y \qquad \Phi\, cos(\theta - \Phi)\,]\ \sigma(r)\, r\ d\theta}{[x^2 + y^2 + \ 4 \qquad - 2r(x^2+y^2)^{1/2} cos(\theta - \Phi)]^{3/2}} = 0$$

If the singular solution is y=0 $\quad (2'') \quad m\frac{d^2 0}{dt^2} + C(z)\left(\frac{d0}{dt}\right)^n - \int_0^{\infty} dr \int_0^{2\pi} \frac{[\, 0 - r\, sin0\, cos(\theta - 0)\,]\ \sigma(r)\, r\ d\theta}{[x^2+0^2+z^2+r^2-2r(x^2+0^2)^{1/2} cos(\theta-0)]^{3/2}} = 0$

As a feature of these equations, although the singular solution y=0 of the mechanical energy stable path holds, it is no longer an even function of y. Also, $\boldsymbol{x = V_x t}$, $\boldsymbol{y = 0}$, $\boldsymbol{z = z_e}$ **hold at** $\boldsymbol{t}$**=∞** and **it passes through the origin point (0, 0, $\boldsymbol{z_0}$).**

(z_e is the solution of $\quad C(z_e)\left(-V_z(z_e)\right)^n + G(z_e) = 0 \quad$)

(z_0 is the solution of $\quad z_0 \int_0^{\infty} dr \int_0^{2\pi} \frac{\sigma(r)\, r\ d\theta}{[(r\, cos\theta)^2 + z_0{}^2]^{3/2}} = G(z_0)$)

As a result, **the stable path is a horizontal straight line at downwind and upwind locations far from the origin.**

Photo 1: Seismic clouds extending eastward over Nara City on January 12, 1978, two days before the Izu Oshima Island Earthquake (M7.0), 330km away upwind. (Photo by Chuzaburo Kamata)

2-2. Equations of motion at the time of calm

At the time of calm, it is temporarily $V_x = V_y = 0$, and the equation of motion at the time of calm is as follows in polar coordinates.

radius ρ direction $\quad m\frac{d^2\rho}{dt^2} + C(z)\left(\frac{d\rho}{dt}\right)^n - \int_0^{\infty} dr \int_0^{2\pi} \frac{\rho\, \sigma(r)\, r\ d\theta}{[\rho^2 + z^2 + r^2 - 2\rho r cos(\theta - \varphi)]^{3/2}} = 0$

circumferential angle φ direction $\quad m\rho\frac{d^2\varphi}{dt^2} + C(z)\left(\rho\frac{d\varphi}{dt}\right)^n = 0$

z direction $\quad m\frac{d}{dt}\left(\frac{dz}{dt} - V_z(z)\right) + C(z)\left(\frac{dz}{dt} - V_z(z)\right)^n + G(z) - \int_0^{\infty} dr \int_0^{2\pi} \frac{z\, \sigma(r)\, r\ d\theta}{[\rho^2 + z^2 + r^2 - 2\rho r cos(\theta - \varphi)]^{3/2}} = 0$

According to mathematical considerations, when there is no wind in the horizontal direction, **the mechanical energy stable path is the singular solution $\boldsymbol{x = y = 0}$ ($\boldsymbol{\rho = 0}$), a vertical line.**

By balancing static forces in the z-axis direction, the equilibrium height z_e of the path is the solution of the following equation.

$$C(z_e)\left(-V_z(z_e)\right)^n + G(z_e) - 2\pi\, z_e \int_0^{\infty} \frac{\sigma(r)\, r\ dr}{[\, z_e{}^2 + r^2]^{3/2}} = 0$$

Photo 2 ; Upright cloud occurred on the evening of Jan.9,1995 taken directly above Akashi-Kaikyo Bridge in the epicenter vicinity one week before the Hyogo South Earthquake (M7.3), (Courtesy of Ms.T. Sugie, NEWS Post Seven) 〔9〕

3. Formation of seismic clouds

Although the charge behavior in the ground and on the surface is not yet clear, according to the internet "A Study on Electrostatic Phenomena and Short-Term Prediction of Earthquakes", the charge on the surface can be interpreted as follows.

The charge can only exist on the surface of the conductor so as to keep the potential inside the conductor constant. When contact friction charging occurs due to continuous deformation strain of the bedrock or fluid friction charging due to the entry of high-pressure fluid into the bedrock (crack) deep underground, positive and negative static electric charge is generated continuously for time. Since the earth's crust can be regarded as a conductor with resistance, both bedrock and fluid conduct electricity and the charge of a conductor generated in the ground can only exist on the surface (when free electrons are stationary) and then the charge rises, and the charge distribution continuously appears on the surface.

When a fluid enters the bedrock deep underground, a charge distribution appears on the surface directly above it. For example, the charge distribution shows such that a negative appears directly above the fluid and a positive appears around it (just above the bedrock), but in this case, the positive charge neutralizes the negative charge on the crustal surface.[10]

Since there is an infinite number of positively and negatively charged water vapor in the air [11], the large negative charge from the ground in the convex part of the land area exerts the Coulomb force and a lot of water vapor condenses close to the path with minimum mechanical energy that is less susceptible to disturbances. As a result, two type (horizontal and vertical) seismic clouds are formed here.

In conclusion, "Many kinds of clouds are formed when the air temperature drops due to the movement of air currents, etc., and water vapor (gas) condenses into water droplets and ice droplets. Seismic clouds are formed when electrically charged water droplets (liquids) floating in the air are subjected to air resistance and Coulomb force and converge on the same streamline.

4. Earthquake source prediction by electric field (or micro-potential) measurement

Prediction of the epicenter by condensation clouds of moisture in the air is considered insufficient because it is limited by weather conditions and land area. On the other hand, a simple electrostatic field compass will be installed at two underground observation points, such as mine shafts and caves that have little influence on the ground. It can be inferred that the intersection of the maximum electrostatic field directions is a very rough epicenter.

Sensor kits in the upper black box.

Metal shell balls in each corner of compass

Metal Shell Ball and Kit Box (Osaka Univ. developed).

Fig. 5 A model of twelve directions electrostatic field compass

In the electrostatic field (or micro-potential) orientation method, precise zero-point adjustment or sensitivity adjustment of the measuring instrument is not required, but only the orientation is the problem.

As shown in the concept of an electrostatic field (or micro-potential) compass (Fig. 5), the electric field (or micro-potential) compass box is surrounded by a fan-shaped metal plate that opens only in one direction, and the metal shell sphere receives the electric field from one direction, and the metal plate shields the electric field from the other direction. The measurement principle is the same for both electrostatic field measurement and micro-potential measurement.

Not only the front of the opening of the azimuth box, but also the line of incidence from the oblique direction hits the shell ball Therefore, the electric field strength of the azimuth box adjacent to the maximum electrostatic field azimuth box is also considered. By means of doing so, the electric field direction can be estimated in detail.

5. Estimation of the timing of an earthquake

When an external force acts on a rock, an electric charge is generated around the crack in the rock, and the crack pops and the charge energy is released, resulting in electromagnetic waves. However, observations of seismic clouds and radio noise [12] indicate that this charge is generated in the early stages of rock strain, several months before the catastrophic earthquake. Considering the social and economic impact on the earthquake and tsunami area, it is desirable to give several days advance notice of the timing of the earthquake. Just before the earthquake (a few days before), a large amount of rock cracks occurred, and the crack sound can be observed as acoustic emission AE, leading to material destruction [13]. In order to detect the sound of cracks deep underground, discarded geothermal generation wells, oil drilling wells (about 1,000 m deep) and foundation piles for offshore wind power generation can be used as elastic wave guides.

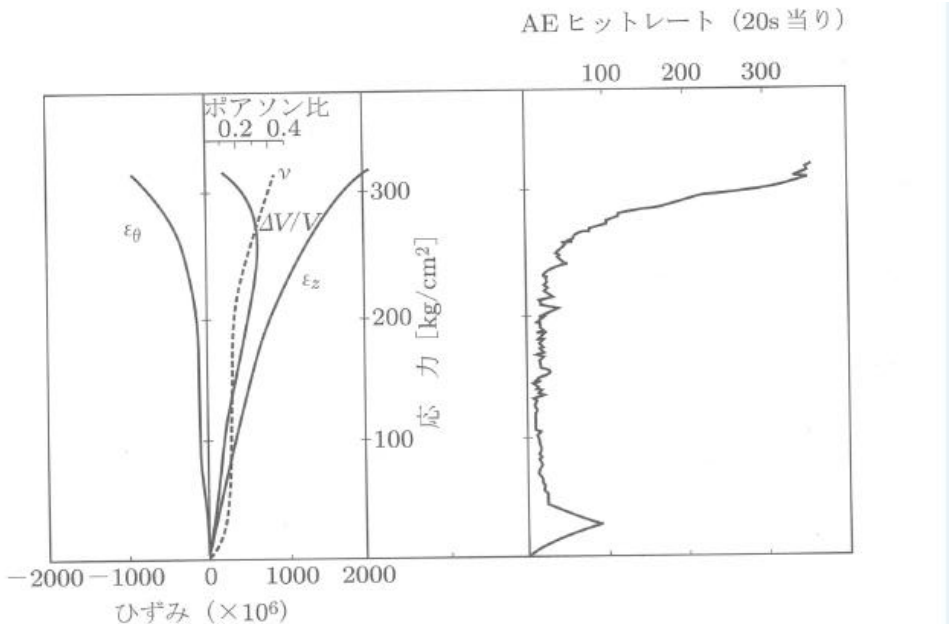

Fig. 6,7 Stress-strain curve and frequency of AE occurrence in uniaxial compression test of concrete specimen

To change the subject, the chemical bond state of water molecules is covalent, and the arrangement bond angle of the hydrogen atoms is 104.5°, which is a folded linear arrangement. This is due to the tetrahedral structural balance of two pairs of shared electrons in the hydrogen atom and two pairs of unshared electrons in the oxygen atom. In this way, the two hydrogen atoms are close to one side, and the hydrogen atom side is

positive and the oxygen atom side is negative. Taking advantage of this property, there is an experiment in which a water stream bends when a plastic baseball pad charged with static electricity is brought close to the water flowing in a thin strip from the faucet. The same is true for water is not a liquid, but a solid of fine oyster ice. This is a type of inverse piezoelectric effect.

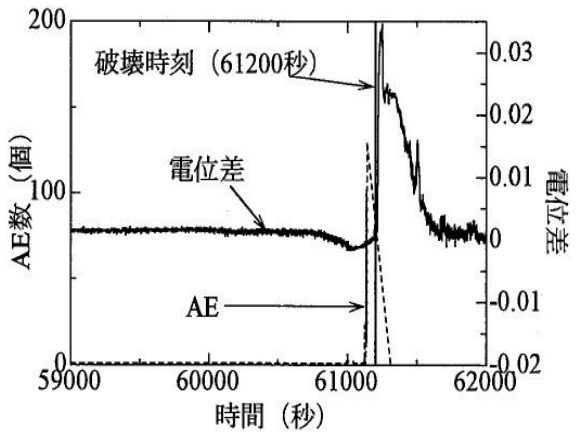

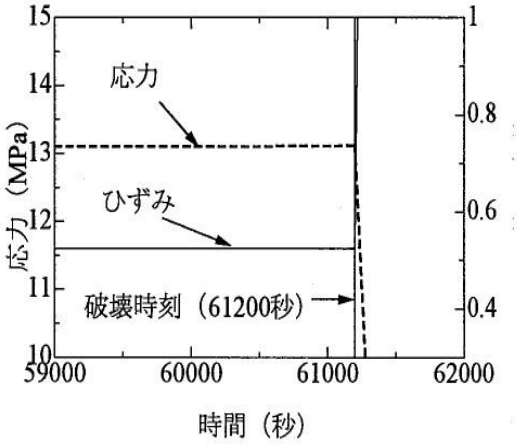

Fig 8 potential-AE-time curve 〔14〕 Fig 9 stress-strain-time curve (Otani stone)

The physical piezoelectric effect is caused by asymmetry in the crystal structure, and when pressure is applied, the force deforms the crystal lattice, resulting in the shift of the positive and negative charge centers in the crystal, and an external voltage is generated. Electric potential generation occurs at the time of elastic deformation, which is the initial stage of material deformation, and elastic wave AE in the plastic deformation region, which is the intergranular fracture and intragrain fracture of the material, has not yet been generated. In the case of rocks, AE tends to occur before material failure[14]. In this sense, the AE method is in principle superior to the electric field and potential measurement method in predicting the imminent occurrence of an earthquake.

6. Simultaneous assumption of the epicenter and occurrence time of an earthquake

When a continuously increasing external force acts on a rock, it occurs as a chronological phenomenon

① Rocks are elastically deformed.

② With elastic deformation, an electric charge is generated by the piezoelectric effect. (Approximately 5~10 days before the earthquake)

③ When the elastic deformation range is exceeded, plastic deformation begins.

④ AE (*p* wave and *s* wave) of elastic waves is generated due to the fracture phenomenon inside the rock. (Approximately 2~3 days before the earthquake)

⑤ Internal destruction progresses slowly, and at some point trigger, the destruction runs out of control, leading to material destruction.

⑥ When a material is destroyed, a lot of conventional electric charge and AE (P and S waves) are released.

⑦ The low ground rumbling during an earthquake is caused by this P wave, and the subsequent shaking is due to the surface wave (or S wave).

As a challenge, the weak elastic waves (*p* wave and *s* wave) of ④ are noise-canceled and digitally measured with a piezoelectric sensor. If this is achieved at three points, 4. directional measurement will be unnecessary. Seismic observation and analysis technology has advanced in isolation since 100 years ago.

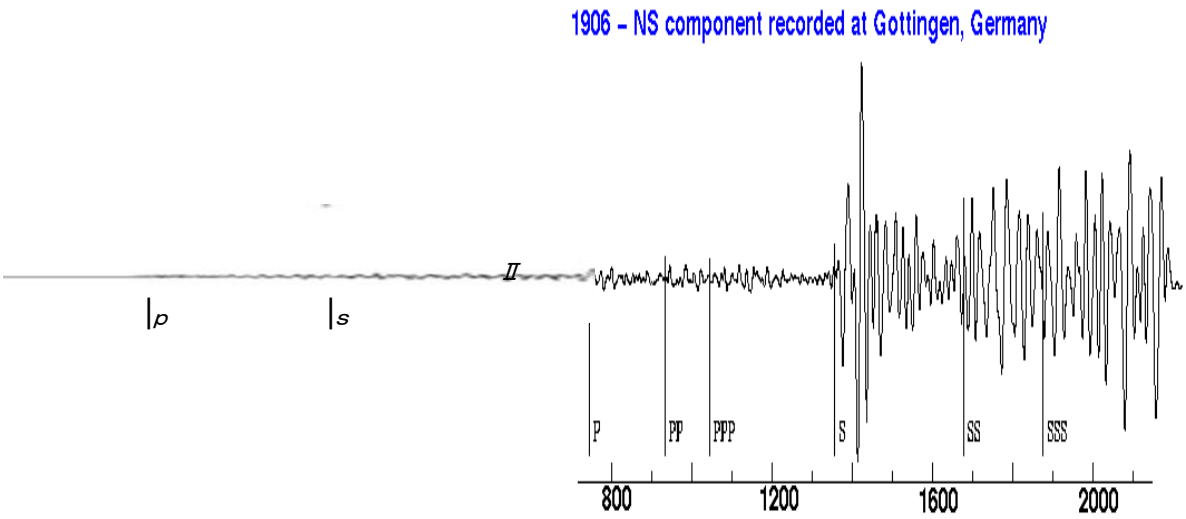

Fig 10 Expected seismic waveform

1906 San Francisco Earthquake was observed in Göttingen, Germany [15].

Micro AE is added to the front of the waveform

References

[1] Series Learning from the Great Hanshin-Awaji Earthquake: Earthquake Prediction and Signs, Journal Isyoshi Vol.38No.12 (1997), Umikiyo Hirohara (Okayama Univ. of Science) 【JPN】

[2] Internet Earthquake Prediction and Omen, Tani Michiyoshi 2005/9/11 Search 【JPN】

[3] Elucidation of the mechanism of rupturing-induced electromagnetic phenomena in rocks - KAKEN Tsutsumi Akito (Kyoto Univ.) http://kaken.nii.ac.jp/ja/.../KAKENHI-PROJECT-13640459/

[4] Mechanism of Ground Surface Charge Generation during Earthquakes IEEJ, Vol. 117, No. 10 C (1997) Takeuchi, Nakahachi (Tohoku Univ.) 【JPN】

[5] Theory of surface plasma waves caused by electric charges generated as precursors to earthquakes, Masafumi Fujii (Univ. of Toyama) 【JPN】

[6] www. Standard atmosphere: Formulas for calculating temperature, pressure, density, sound velocity, viscosity coefficient, and kinematic viscosity coefficient of air at each altitude

[7] www.city.nagoya.jp/.../48Jhyoka_shiryo_01_02.pdf, Average wind speed vertical distribution by altitude,

[8] Official Handbook of Higher Mathematics Trans. Kawamura and Imoto, Asakura 2013 【JPN】

[9] There is "no scientific basis" for the "seismic clouds" witnessed in the Great Hanshin-Awaji 【JPN】 Internet Earthquakewww.news.yahoo.co.jp/.../525a9287cf4ecb98402daf1488d4c... 2023/9/1 search

[10] Internet "A Study on Electrostatic Phenomena and Short-term Prediction of Earthquakes"2023/9/1 search【JPN】

[11] Introduction to Atmospheric Electricity p143, The Japan Society of Atmospheric Electricity, Coronasha, 2003

[12] Internet Reverse Radio Earthquake Prediction Research - Electromagnetic Wave Noise Detection Analysis

[13] Characteristics and Theory of Acoustic Emission [2nd Edition] Masayasu Otsu p28 Morikita Shuppan 2005

[14] Study on Potential Generation Behavior in the Creep Deformation Process of Rocks Tomoyuki Akagi Toyota National College of Technology 2004

[15] Internet USGS 1906 San Francisco Earthquake - Shaking at Gottingen, Germany 2023/9/1 search

Declarations

Acknowledgements

This research did not receive any specific grant from funding agencies in the public, commercial, or not-for-profit sectors. The author declares no competing interests including financial and non-financial interests.

Author Contributions

F. I. developed the theory and wrote the manuscript.